

## **Supplementary Information - Automated Discovery of Noncovalent Inhibitors of SARS-CoV-2 Main Protease by Consensus Deep Docking of 40 Billion Small Molecules**

Francesco Gentile<sup>a</sup>, Michael Fernandez<sup>a</sup>, Fuqiang Ban<sup>a</sup>, Anh-Tien Ton<sup>a</sup>, Hazem Mslati<sup>a</sup>, Carl F. Perez<sup>a</sup>, Eric Leblanc<sup>a</sup>, Jean Charle Yaacoub<sup>a</sup>, James Gleave<sup>a</sup>, Abraham Stern<sup>b</sup>, Bill Wong<sup>c</sup>, François Jean<sup>d</sup>, Natalie Strynadka<sup>e</sup>, and Artem Cherkasov<sup>a\*</sup>

*<sup>a</sup>Vancouver Prostate Centre, Department of Urologic Sciences, The University of British Columbia, Vancouver, BC, Canada*

*<sup>b</sup>NVIDIA Corporation, Santa Clara, CA, United States*

*<sup>c</sup>Dell Canada, North York, ON, Canada*

*<sup>d</sup>Department of Microbiology and Immunology, The University of British Columbia, Vancouver, BC, Canada*

*<sup>e</sup>Department of Biochemistry and Molecular Biology, The University of British Columbia, Vancouver, BC, Canada*

*\*Corresponding author: Vancouver Prostate Centre, 2660 Oak Street, Vancouver, British Columbia, V6H3Z6, Canada, acherkasov@prostatecentre.com*

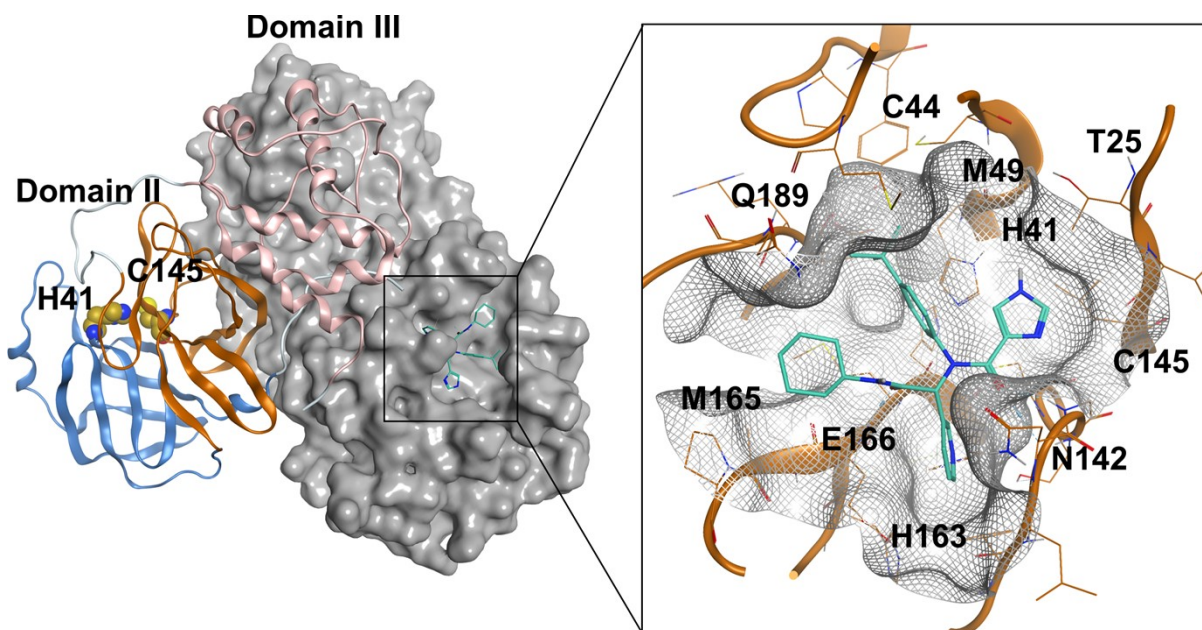


**Figure S1.** Dimeric structure of SARS-CoV-2 Mpro bound to X77 (from PDB:6W63), with a focus view of the active site.

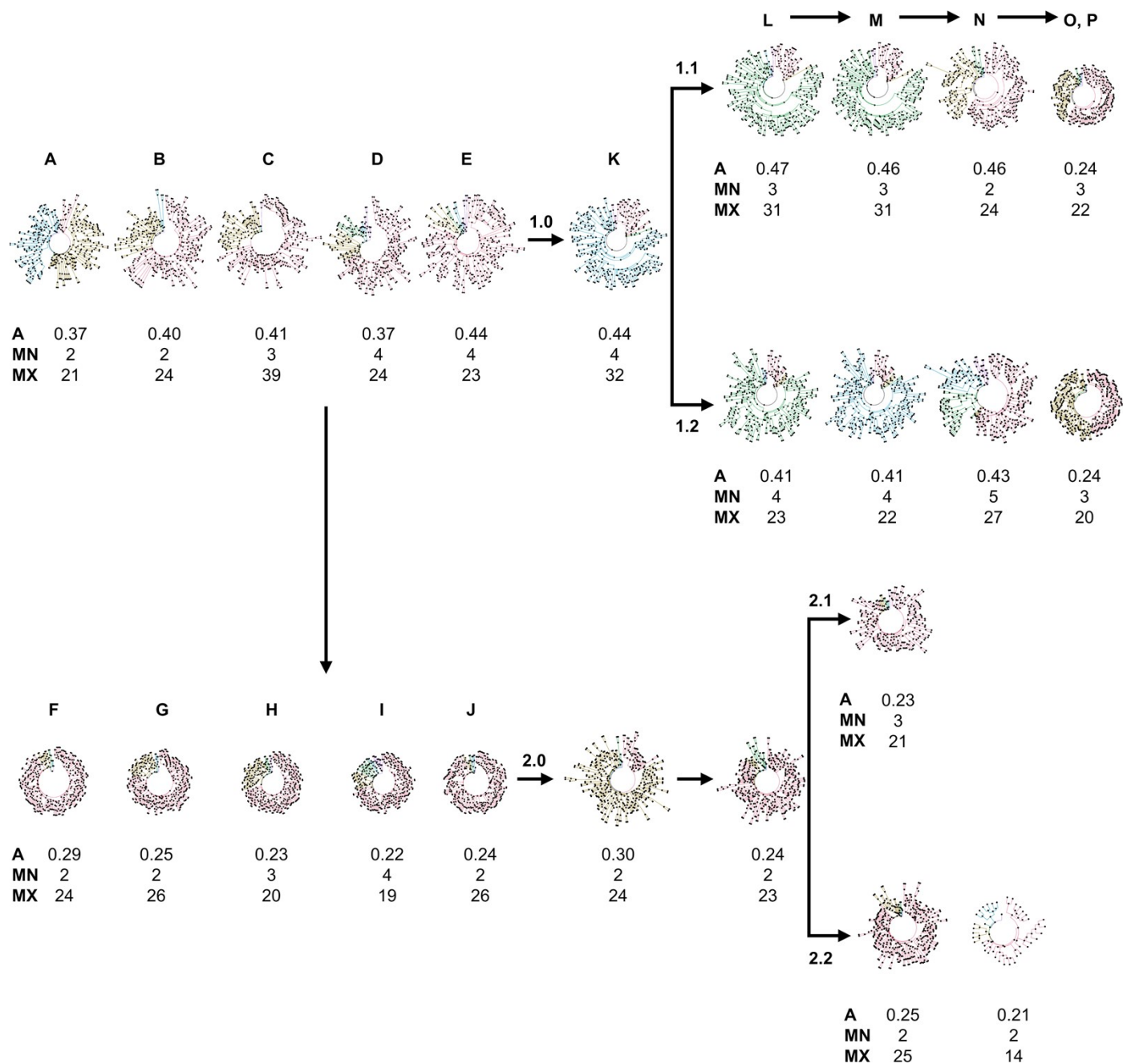
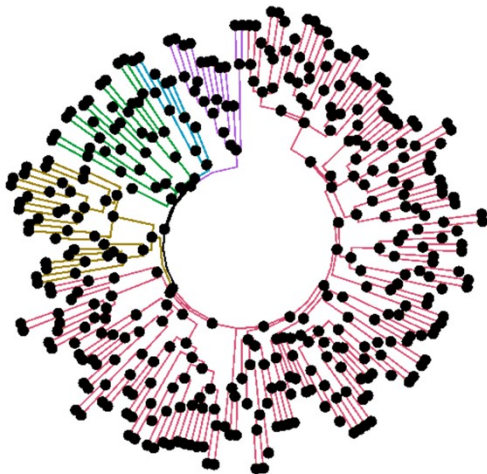
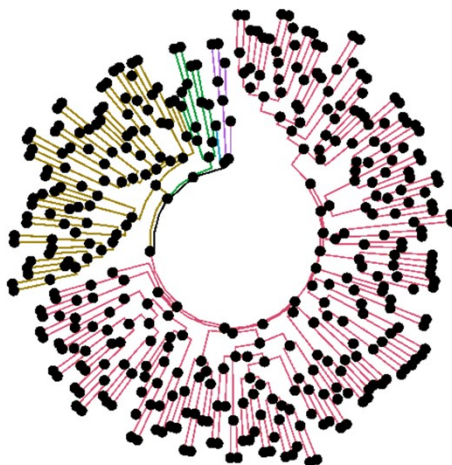


**Figure S2.** Tanimoto-based hierarchical agglomerative clustering of top-100 compounds returned by each selection strategy. Below each circular dendrogram, the corresponding agglomerative coefficient (A), minimum (MN) and maximum (MX) number of nodes are reported.

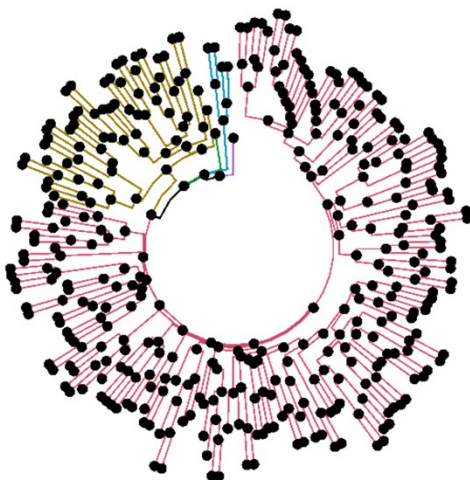
a



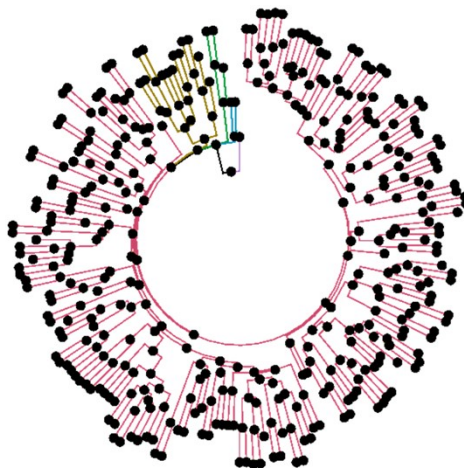
b



c



d



e

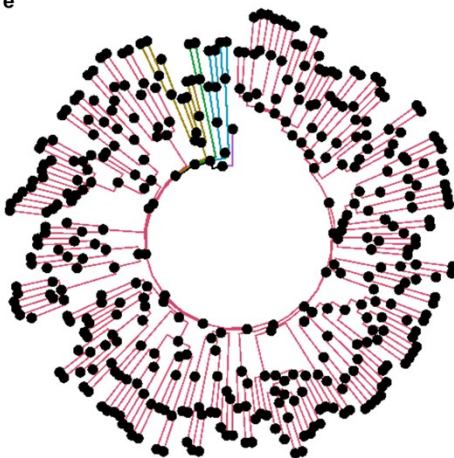


**Figure S3.** Tanimoto similarity trees of top-100 compounds from individual docking programs after chemical diversity selection, where the top-five clusters are highlighted by different colors in each dendrogram. **a**, Autodock GPU, **b**, Glide SP, **c**, FRED, **d**, ICM and **e**, QuickVina2.

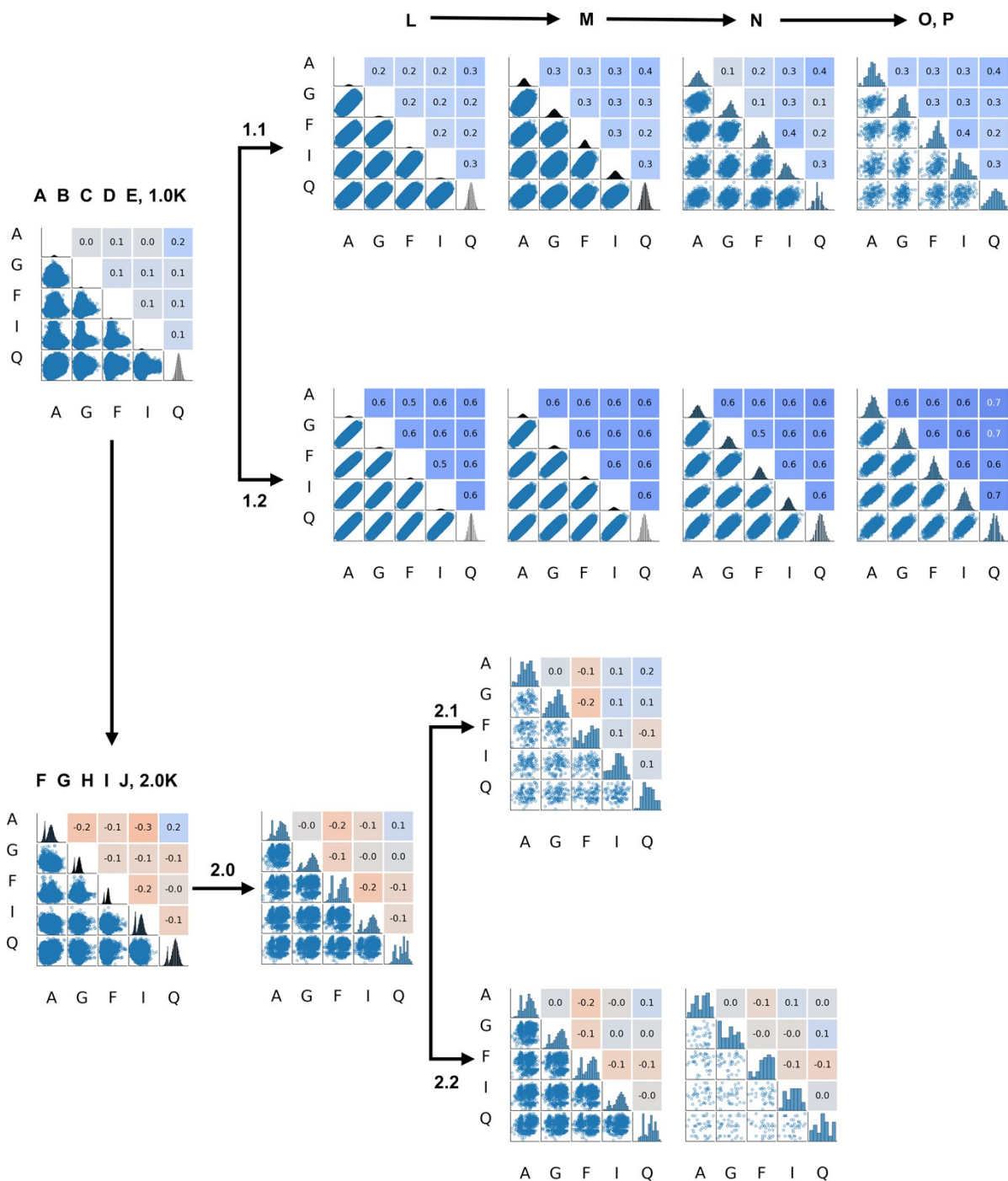


**Figure S4.** Correlation of docking scores for different hit selection strategies. Score distributions, correlation plots and Pearson coefficients between individual docking scores for the twenty-six filtering strategies.



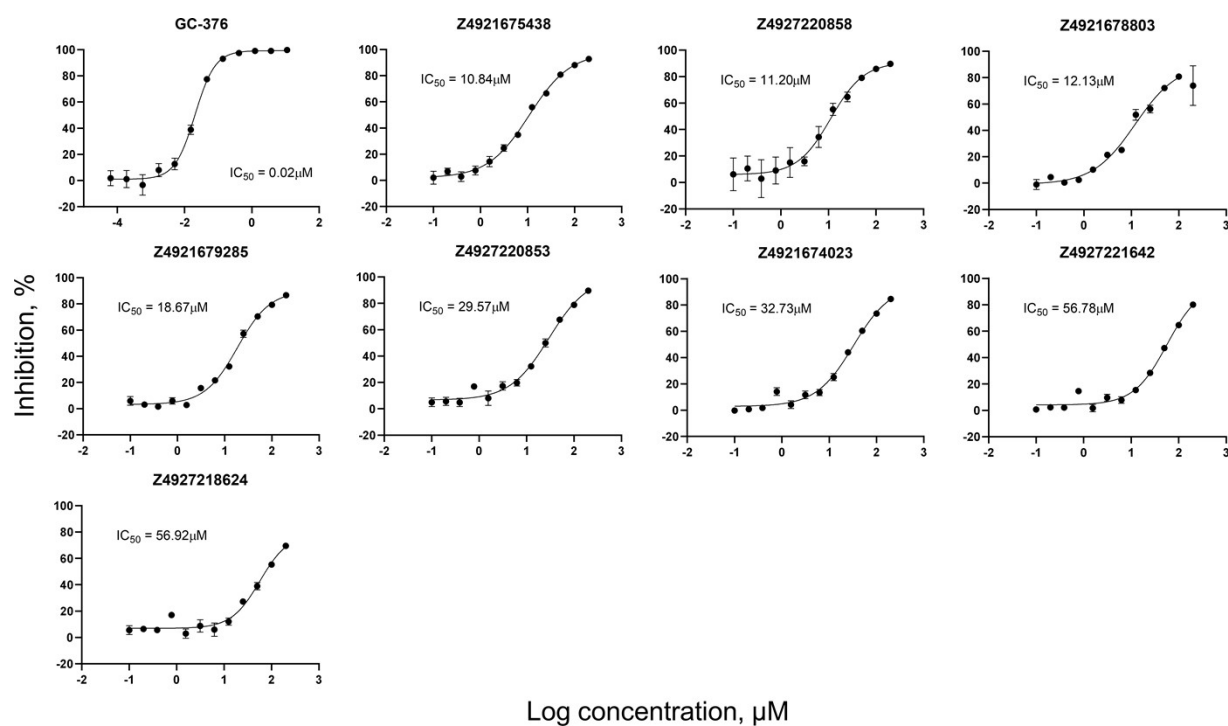


**Figure S5.** Dose-response curves and measured  $\text{IC}_{50}$  for control compound (GC-376) and eight identified inhibitors with  $\text{IC}_{50}$  values below 100  $\mu\text{M}$ .